Hopf bifurcation analysis and circuit implementation for a novel four-wing hyper-chaotic system*

Xue Wei(薛 薇)[a)†], Qi Guo-Yuan(齐国元)[b)‡], Mu Jing-Jing(沐晶晶)[a)],
Jia Hong-Yan(贾红艳)[a)§], and Guo Yan-Ling(郭彦岭)[b)]

[a)] *Department of Automation, Tianjin University of Science & Technology, Tianjin* 300222, *China*
[b)] *F'SATI/Department of Electrical Engineering, Tshwane University of Technology, Pretoria* 0001, *South Africa*

(Received 12 November 2012; revised manuscript received 16 January 2013)

In the paper, a novel four-wing hyper-chaotic system is proposed and analyzed. A rare dynamic phenomenon is found that this new system with one equilibrium generates a four-wing-hyper-chaotic attractor as parameter varies. The system has rich and complex dynamical behaviors, and it is investigated in terms of Lyapunov exponents, bifurcation diagrams, Poincaré maps, frequency spectrum, and numerical simulations. In addition, the theoretical analysis shows that the system undergoes a Hopf bifurcation as one parameter varies, which is illustrated by the numerical simulation. Finally, an analog circuit is designed to implement this hyper-chaotic system.

Keywords: hyper-chaos, four-wing chaotic system, one equilibrium, Hopf bifurcation, circuit implementation

PACS: 05.45.–a, 05.45.Pq **DOI:** 10.1088/1674-1056/22/8/080504

1. Introduction

Since Lorenz discovered the first chaotic attractor in 1963[1] and the Rössler hyper-chaotic attractor was obtained by computer simulation in 1979,[2] more and more scholars have shown their interest in the research on generation, analysis, synchronization, and control of chaos and hyper-chaos. The research on chaos and hyper-chaos has become a hotspot. In the last decade, many researchers have employed different techniques such as Lyapunov exponent, Poincaré mapping, and topological horseshoe, etc. to analyze some chaotic systems, such as Qi systems,[3,4] Chen system,[5] Lü system,[6] multi-wing system,[7–14] and fractional-order chaotic system.[15–17] Many scholars have also generated and analyzed some hyper-chaotic systems,[18–24] and the research on circuit implementations and applications of some chaotic systems has been conducted as well.[25–34]

Since a hyper-chaotic system with two or more positive Lyapunov exponents expands in two or more directions, it complicates dynamical behaviors, which offers it a broader application value than a normal chaotic system in some domains, such as communication encryption and image encryption.[35–37] To achieve a hyper-chaotic attractor, a continuous autonomous system must have at least four dimensions, and there must be two unstable items in the coupled equations of the system, one of them must be nonlinear. Although much work has been done in the generation and analysis of hyper-chaotic systems,[18,30] it is still an interesting thing to generate multi-wing hyper-chaotic systems with simple mathematical model and complex dynamic behavior.

Circuit implementation not only verifies the existence of hyper-chaos in the physical sense, but also promotes the application of the hyper-chaos. If a hyper-chaotic system can be implemented by an analog circuit, then it will also be easier to be adopted in confidential communication. For some systems, circuit implementation and application research have been performed.[25–30,34]

In the present paper, we construct a four-dimensional continuous autonomous hyper-chaotic system by adding a linear feedback controller to the Qi four-wing chaotic system.[3] The system has three nonlinear items and only one equilibrium point. Despite only one equilibrium point, it possesses a four-wing hyper-chaotic attractor. The basic dynamic characteristics and bifurcation of an attractor are analyzed in terms of phase diagrams, Lyapunov exponent spectrum, bifurcation diagram, Poincaré mapping, and frequency spectral analysis. These analyses indicate that the new system possesses very

*Project supported by the National Natural Science Foundation of China (Grant Nos. 10772135 and 60874028), the Young Scientists Fund of the National Natural Science Foundation of China (Grant No. 11202148), the Incentive Funding of the National Research Foundation of South Africa (Grant No. IFR2009090800049), the Eskom Tertiary Education Support Programme of South Africa, and the Research Foundation of Tianjin University of Science and Technology.

†Corresponding author. E-mail: xuewei@tust.edu.cn
‡Corresponding author. E-mail: qig@tut.ac.za
§Corresponding author. E-mail: jiahy@tust.edu.cn

© 2013 Chinese Physical Society and IOP Publishing Ltd

complicated dynamic characteristics, and it is even more interesting that a broad range of hyper-chaos can be observed when the parameter is varied. Finally, an analog circuit is built to implement the new hyper-chaotic system. The output portraits of the circuit fit to the results of theoretical analysis and numerical simulation, thereby verifying the hyper-chaotic attractor at a physical level and providing a technical foundation for further actual application.

2. Novel hyper-chaotic system and its basic properties

Qi *et al.*[11] reported on a three-dimensional (3D) four-wing chaotic system, which is described as

$$\begin{cases} \dot{x} = a(y-x) + eyz, \\ \dot{y} = cx + dy - xz, \\ \dot{z} = -bz + xy, \end{cases} \tag{1}$$

where a, b, d, e, $f \in R^+$, $c \in R$. On the basis of the above Qi system, a novel system is obtained by adding a linear feedback control as follows:

$$\begin{cases} \dot{x} = a(y-x) + eyz, \\ \dot{y} = cx + dy - xz - w, \\ \dot{z} = -bz + xy, \\ \dot{w} = fy, \end{cases} \tag{2}$$

where a, b, d, $e \in R^+$, c, $f \in R$, are constant parameters of the system, with f being a parameter determining the chaotic or hyper-chaotic behaviors and bifurcations of system (2).

2.1. Equilibria

In order to obtain the equilibrium of system (2), let $\dot{x} = \dot{y} = \dot{z} = \dot{w} = 0$, i.e.,

$$\begin{cases} a(y-x) + eyz = 0, \\ cx + dy - xz - w = 0, \\ -bz + xy = 0, \\ fy = 0, \end{cases} \tag{3}$$

which determines only one equilibrium at the origin $S_0 = (0,0,0,0)$.

For system (2) Jacobian matrix at $S_0 = (0,0,0,0)$ is obtained as

$$J_0 = \begin{bmatrix} -a & a & 0 & 0 \\ c & d & 0 & -1 \\ 0 & 0 & -b & 0 \\ 0 & f & 0 & 0 \end{bmatrix}, \tag{4}$$

and its characteristic equation is

$$f(\lambda) = (\lambda + b) f_1(\lambda) = 0, \tag{5}$$

where

$$f_1(\lambda) = \lambda\left[\lambda^2 + (a-d)\lambda - ac - ad\right] + f(\lambda + a)$$
$$= \lambda^3 + (a-d)\lambda^2 + (f - ac - ad)\lambda + af.$$

The first eigenvalue is at $\lambda_1 = -b$, according to Routh–Hurwitz criterion, the real parts of the others in $f_1(\lambda) = 0$ are negative if and only if $d < a, c + d < 0$. Furthermore, equilibrium point $S_0 = (0,0,0,0)$ of system (2) is asymptotically stable when $0 < d < a, d < |c|$, $c < 0$, and system (2) has no chaotic or hyper-chaotic attractor.

2.2. Symmetry and dissipation of system (2)

System (2) is symmetric about the z axis, for it is invariant under the coordinate transformation:

$$(x, y, z, w) \to (-x, -y, z, -w). \tag{6}$$

For the new system, let the equation

$$\nabla V = \frac{\partial \dot{x}}{\partial x} + \frac{\partial \dot{y}}{\partial y} + \frac{\partial \dot{z}}{\partial z} + \frac{\partial \dot{w}}{\partial w} = -a + d - b < 0, \tag{7}$$

which means that system (2) is dissipative with an exponential contraction rate

$$\frac{\mathrm{d}V}{\mathrm{d}t} = \mathrm{e}^{-(a+b-d)t}. \tag{8}$$

3. Observation and analysis of the new hyper-chaotic system

3.1. Bifurcation analysis

Lyapunov exponent spectra and bifurcation diagrams of system (2) are shown in Figs. 1 and 2, respectively. From Fig. 1, one can observe that there are two positive Lyapunov exponents over quite a wide range of parameter f, which implies that system (2) is hyper-chaotic over a broad range. The fourth Lyapunov exponent L_4 is less than -30, so it is not shown in Fig. 1. In order to clearly display the rich dynamical behaviors of system (2), namely dynamics of periodic orbit, quasi-periodic orbit, chaos and hyper-chaos and their evolution process, the Lyapunov exponent spectra and bifurcation diagrams are divided into two figure paintings respectively, as shown in Figs. 1(a) and 1(b), and Figs. 2(a) and 2(b). As can be seen from Figs. 1 and 2, system (2) has very rich dynamics. The Lyapunov exponent spectra and bifurcation diagrams are well consistent with the results.

System (2) is in periodic orbit when f is varied in the parameter ranges: [0, 2.3], [8.3, 8.8], [10.9, 12.2], [13.8, 19], [20.2, 21.6], [89.4, 97.5], [225.5, 229.5], [244.8, 289.9], and [295.6, 300]. For example, fixing $f = 16$, the Lyapunov exponents of system (2) are $L1 = 0$, $L2 = -0.8599$, $L3 = -3.6573$, and $L4 = -37.4455$, which indicates that system (2) is a periodic orbit as shown in Fig. 3.

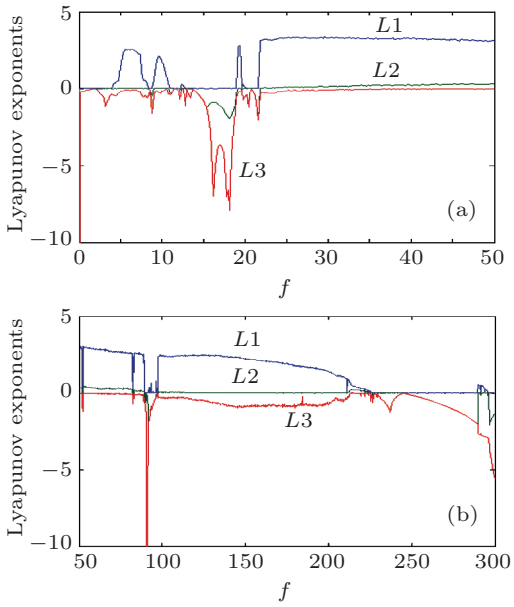


Fig. 1. (color online) Lyapunov exponent spectra when $a = 15$, $b = 43$, $c = -6$, $d = 16$, $e = 5$, f varying from 0 to 300. (a) Lyapunov exponents spectra: f is varied from 0 to 50. (b) Lyapunov exponents spectra: f is varied from 50 to 300.

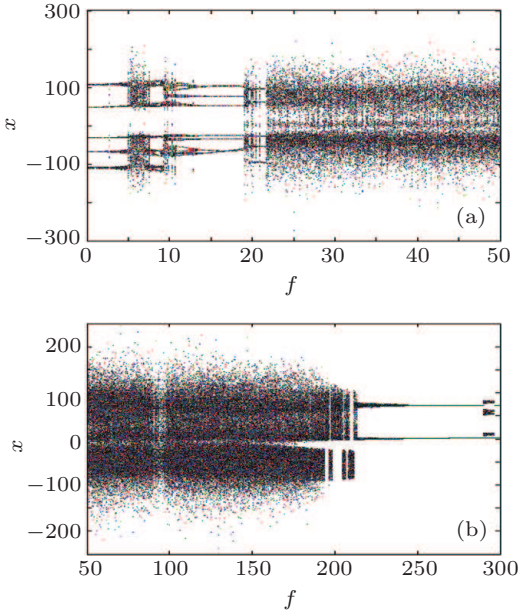


Fig. 2. (color online) Bifurcation diagram when $a = 15$, $b = 43$, $c = -6$, $d = 16$, $e = 5$, f varying from 0 to 300. (a) Bifurcation diagram in x direction: f is varied from 0 to 50. (b) Bifurcation diagram in x direction: f is varied from 50 to 300.

The system is in quasi-periodic orbit, i.e. the first and the second Lyapunov exponent are zeros when f is varied in the parameter ranges: (2.3, 4.1], [12.8, 13.8), and (229.5, 244.8). For example, fixing $f = 240$, $L1 = L2 = 0$, $L3 = -0.3816$, and $L4 = 41.6296$, indicating that it is a quasi-periodic orbit as shown in Fig. 4.

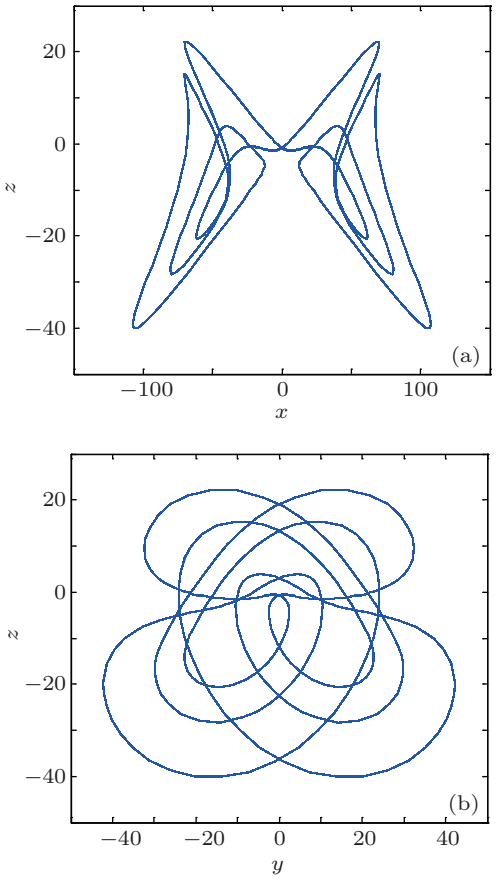


Fig. 3. (color online) System (2) in a periodic state with $a = 15$, $b = 43$, $c = -6$, $d = 16$, $e = 5$, $f = 16$: (a) projections in x–z plane and (b) projection in y–z plane.

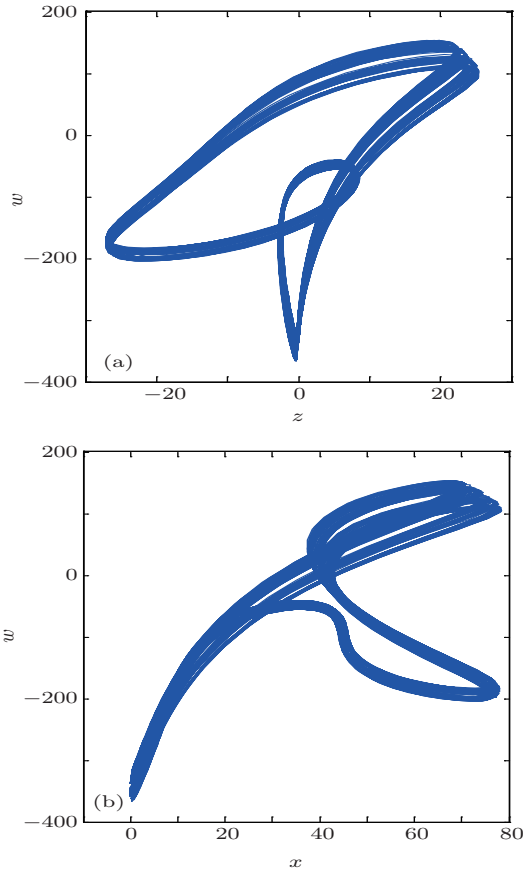


Fig. 4. (color online) System (2) in a quasi-periodic state with $a = 15$, $b = 43$, $c = -6$, $d = 16$, $e = 5$, $f = 240$: (a) projection in z–w plane and (b) projection in x–w plane.

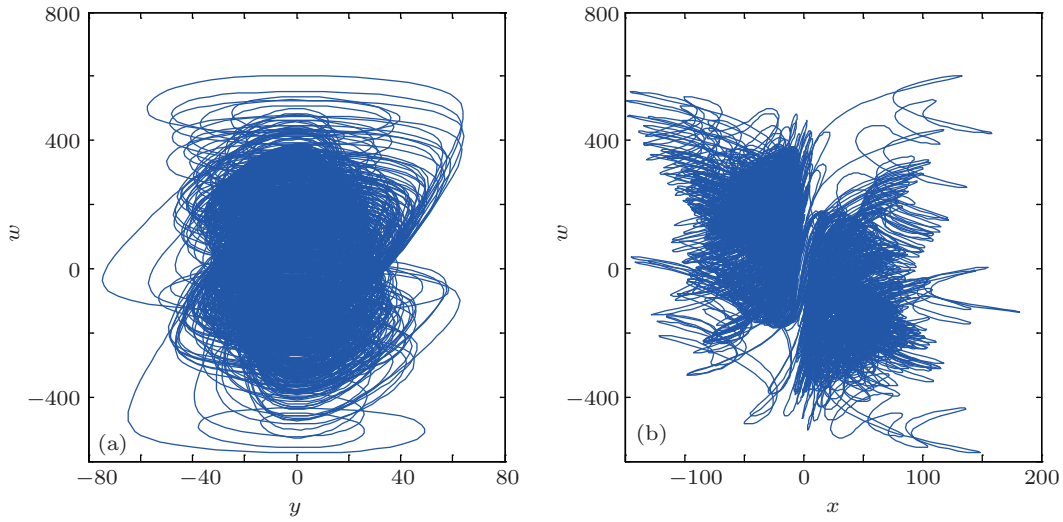


Fig. 5. (color online) System (2) in a four-wing-chaotic state with $a = 15$, $b = 43$, $c = -6$, $d = 16$, $e = 5$, $f = 150$. (a) Projection in y–w plane and (b) projection in x–w plane.

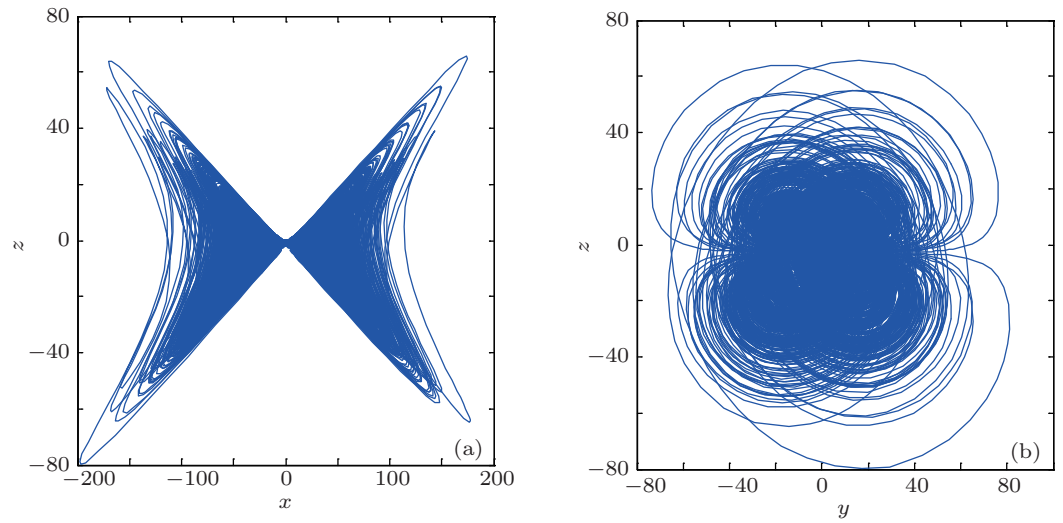


Fig. 6. (color online) System (2) in a four-wing-hyper-chaotic state with $a = 15$, $b = 43$, $c = -6$, $d = 16$, $e = 5$, $f = 60$: (a) projection in y–z plane and (b) projection in x–z plane.

The system is in chaos, when f is varied in the parameter ranges: (4.1, 8.3), (8.8, 10.9), (12.2, 12.8), (19, 20.2), (21.6, 31), (88.2, 89.4), (97.5, 212.9], and (289.9, 295.6). For instance, fixing $f = 150$, it has $L1 = 2.2323$, $L2 = 0$, $L3 = -0.9481$, and $L4 = -43.2707$, indicating that it is a chaotic state as shown in Fig. 5. The attractor has four wings, so it is a four-wing chaotic attractor.

The system is in hyper-chaos when f is varied in the parameter ranges of [31, 88.2] and (212.9, 225.5). For instance, fixing $f = 60$, $L1 = 2.8869$, $L2 = 0.3325$, $L3 = 0$, and $L4 = -45.0744$, indicating that system (2) is in a hyper-chaotic state as shown in Fig. 6. The attractor has four wings, so it is a four-wing-hyper-chaotic attractor, which rarely appears in other chaotic systems.

3.2. Poincaré map

Through the Poincaré map diagram in the x–z plane of Fig. 7(a), it is clearly observed that system (2) has a four-wing attractor. In the x–y plane [Fig. 7(b)], the mapping points are dispersive and disordered. The two diagrams which are in y direction and z direction respectively prove that the system has four wings and is chaotic. In addition, it has two positive Lyapunov exponents, therefore it is definitely a four-wing-hyper-chaotic attractor.

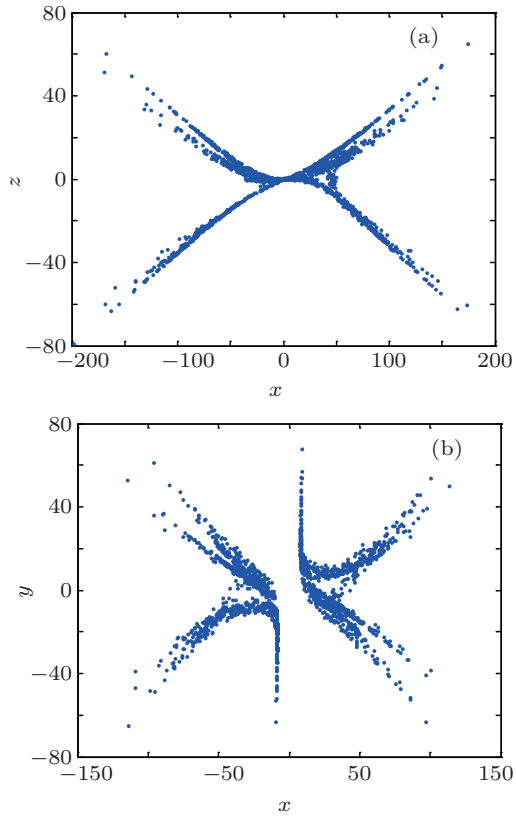


Fig. 7. (color online) Poincaré map diagrams of the system (2) with $a = 15$, $b = 43$, $c = -6$, $d = 16$, $e = 5$, $f = 60$: (a) x–z plane ($y = 6$). (b) x–y plane ($z = 1.5$).

3.3. Frequency spectral analysis

Figure 8 shows the frequency spectrum of system (2) which can generate a four-wing-hyper-chaotic attractor at the parameters $a = 15$, $b = 43$, $c = -6$, $d = 16$, $a = 15$, $b = 43$, $c = -6$, $d = 16$, $e = 5$, $f = 50$. From Fig. 8 it follows that system (2) has a broad frequency bandwidth. Therefore the chaotic signals of system (2) can be used in real communication.

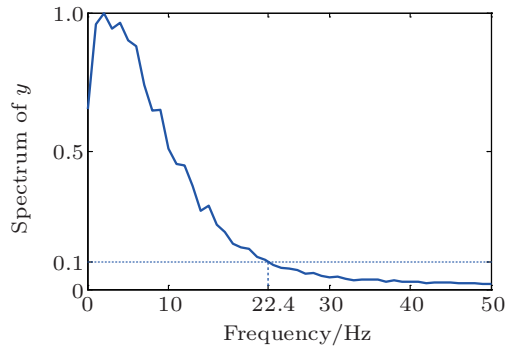


Fig. 8. (color online) Frequency spectrum of system (2).

4. Hopf bifurcation of the system (2)

If the chaotic system has Hopf bifurcation, the vector field must satisfy the following two conditions:[38]

(i) The Jacobian matrix of system at the specified equilibrium has two purely imaginary eigenvalues;

(ii) The real parts of eigenvalues must satisfy

$$\frac{\mathrm{d}}{\mathrm{d}\mu}(\mathrm{Re}(\lambda(\mu)))\big|_{\mu=\mu_0} \neq 0.$$

System (2) may have Hopf bifurcation when parameter f varies. Suppose that $f(\lambda)$ has a pair of pure imaginary roots

$$\lambda = \pm \mathrm{i}\omega_0, \quad \omega_0 \in R^+,$$

then it will be easy to obtain

$$f = f_0 = \frac{a(d+c)(d-a)}{d}, \ d < a, \ c + d < 0. \tag{9}$$

The Jacobian matrix equation (4) of system (2) at origin has two real negative eigenvalues and a pair of imaginary eigenvalues as follows:

$$\lambda_1 = -b, \quad \lambda_2 = -(a-d),$$

and

$$\lambda_{3,4} = \alpha(f_0) \pm \mathrm{i}\omega(f_0) = \pm \mathrm{i}\omega_0,$$

where

$$\omega_0 = \sqrt{f_0 - ad - ac}.$$

i.e. condition (1) is satisfied.

Let

$$\lambda = \alpha(f) + \mathrm{i}\omega(f),$$

and differentiate all the terms of $f_1(\lambda)$ in Eq. (5) with respect to f, then we will have

$$\left.\frac{\mathrm{d}\alpha(f)}{\mathrm{d}f}\right|_{f=f_0} = \left.\frac{-a}{3\alpha^2(f) - 2(a-d)\alpha(f) - 2(f - ac - ad)}\right|_{f_0}$$

$$= \frac{d}{(d+c)(d-2a)} \neq 0, \tag{10}$$

where $a > 0$, $c < 0$, $d > 0$, $c + d < 0$, and $d < a$. Therefore condition (2) is also satisfied. Thus, system (2) undergoes a Hopf bifurcation at equilibrium point $S_0 = (0,0,0,0)$.

With $a = 15$, $b = 43$, $c = -6$, $d = 5$, and $e = 5$, solving Eq. (9) gives $f_0 = 30$. Thus, the eigenvalues are

$$\lambda_1 = -43, \ \lambda_2 = -10, \ \lambda_3 = \mathrm{i}3\sqrt{5}, \ \text{and} \ \lambda_4 = -\mathrm{i}3\sqrt{5}.$$

Furthermore, in a certain range of $f > 30$, system (2) is a periodic attractor; in a certain range of $f < 30$, system (2) is an asymptotically stable attractor, i.e. a sink.

Now select $f = 25$ and $f = 35$, system (2) is an asymptotically stable attractor and a periodic attractor as shown in Figs. 9(a) and 9(b), respectively.

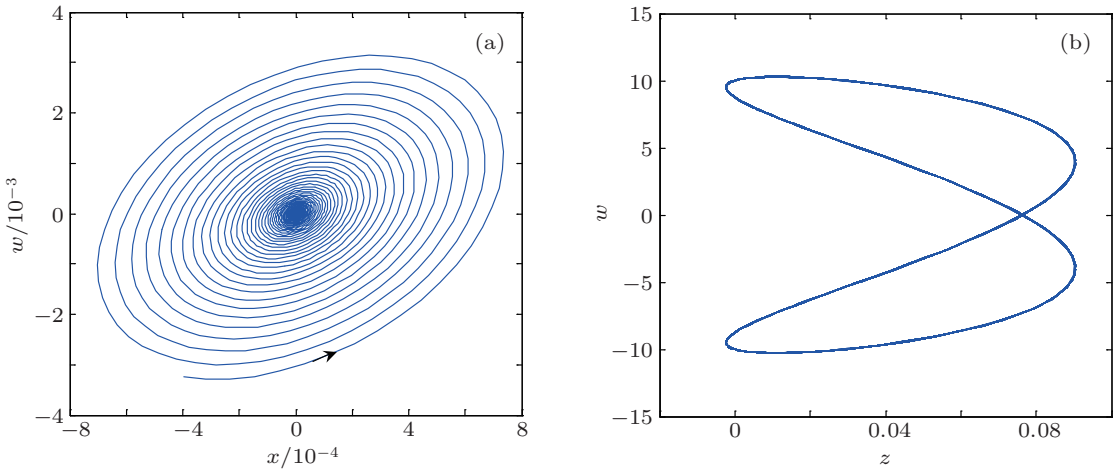


Fig. 9. (color online) phase portraits of system (2) with the parameters: $a = 15$, $b = 43$, $c = -6$, $d = 5$, and $e = 5$. (a) A sink with $f = 25$. (b) A periodic orbit with $f = 35$.

5. Circuit implementation of system (2)

Building circuits serves as the simplest way of physically realizing the hyper-chaotic system and also as an essential means of investigating dynamic characteristic of the hyper-chaotic system. Meanwhile, it also provides the technical support for the hyper-chaotic system applied to some engineering field such as communication security.

First, the system is assumed to have a linear scaling when the actual hardware circuit is built which makes all the variables be within the range of actual hardware circuit voltage allowed. In general, the allowed voltage is in a range between -15 V and $+15$ V. In this paper, all the four state variables of hyper-chaotic system (2) are scaled. The multiples of scale are as follows: $x = 20$, $X = 20Y$, $z = 20Z$, $w = 50W$, respectively. Substituting these into equations of hyper-chaotic system (2), we can obtain

$$\begin{cases} 0.1\dot{X} = 0.1a(Y - X) + 2eYZ, \\ 0.1\dot{Y} = 0.1cX + 0.1dY - 2XZ - 0.25W, \\ 0.1\dot{Z} = -0.1bZ + 2XY, \\ 0.1\dot{W} = 0.04fY. \end{cases} \tag{11}$$

After scaling, system (11) is similar to the original hyper-chaotic system (2).

According to system (11), a chaotic circuit with four coupling channels is designed in this paper, which is shown in Fig. 10. From top to bottom, each part represents variable x, y, z, and w sequentially. Analogue amplifier LF347N is used in the circuit to realize the function of addition, subtraction, and integral operations. The multiplier with its model number AD633JN is used in outputting nonlinear terms. The modulus of the multiplier is 0.1, which should be considered when calculating circuit parameters.

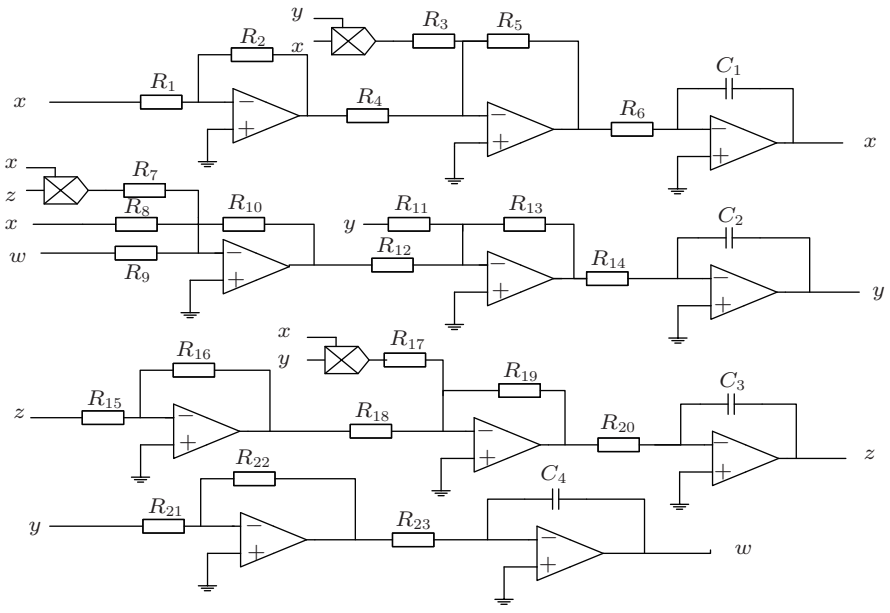


Fig. 10. Diagrams of circuitry implementation of system (2).

Circuit parameters in Fig. 10 are as follows: $R_1 = R_4 = R_5 = R_6 = R_8 = R_{11} = R_{14} = R_{15} = R_{18} = R_{19} = R_{20} = R_{22} = R_{23} = 100$ kΩ, $R_2 = 150$ kΩ, $R_3 = 10$ kΩ, $R_7 = 30$ kΩ, $R_9 = 240$ kΩ, $R_{10} = 60$ kΩ, $R_{12} = R_{13} = 160$ kΩ, $R_{16} = 430$ kΩ, $R_{17} = R_{21} = 50$ kΩ, $C_1 = C_2 = C_3 = C_4 = 10$ nF, and R_{21} is adjustable resistor. By regulating R_{21}, the value of parameter f is changed correspondingly.

The arithmetic product of coefficient RC in integral circuit is 100 kΩ × 10 nF = 10^{-3}, and the corresponding frequency is improved 100 times. After the transformation, the amplification of the system and the coefficient of the integral circuit are both suited to observe the phase tracks of chaotic and hyper-chaotic attractor of the system on an analog oscilloscope instantly. The circuitry implementation diagram and circuitry results are shown in Figs. 10 and 11, respectively. One can see that the observations of physical implementation match the numerical simulations of the phase portrait, i.e., figures 11(a1) and 11(a2) correspond to Figs. 3(a) and 3(b), respectively, Figs. 11(b1) and 11(b2) to Figs. 5(a) and 5(b), respectively, and Figs. 11(c1) and 11(c2) to Figs. 6(a) and 6(b), respectively.

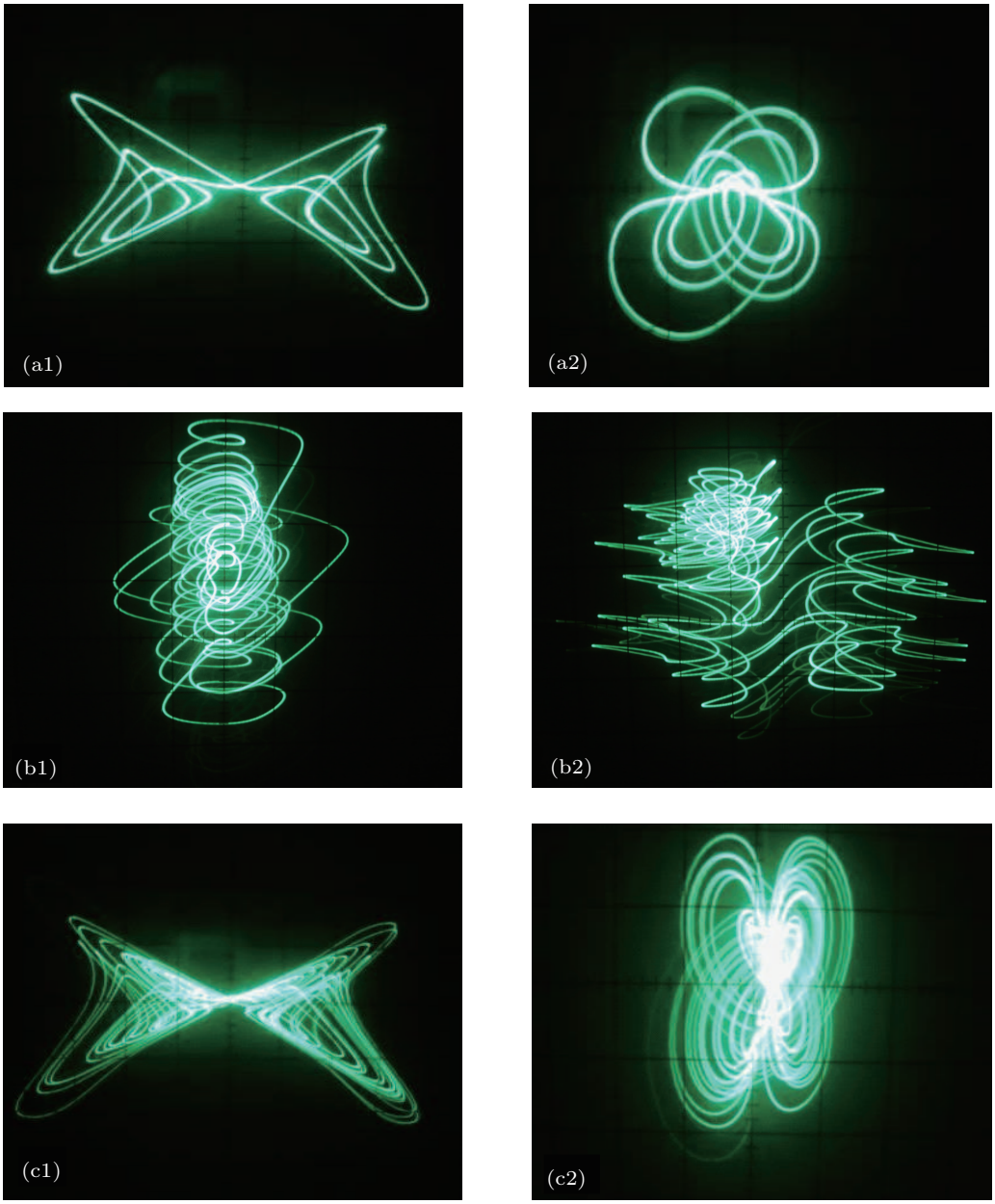


Fig. 11. (color online) Phase portraits of chaotic system (2) observed on an analog oscilloscope YB4325 with $a = 15$, $b = 43$, $c = -6$, $d = 16$, $e = 5$. (a) A periodic attractor when $f = 16$. (b) A four-wing-chaotic attractor when $f = 150$. (c) A four-wing-hyper-chaotic attractor when $f = 60$.

6. Conclusions

In this paper, a new hyper-chaotic system is obtained by adding a linear controller produced by the additional fourth equation to the second equation of a three-dimensional autonomous Qi four-wing chaotic system. This hyper-chaotic system with only one equilibrium point can demonstrate both hyper-chaotic and four wing hyper-chaotic behaviors in a large range of parameter space. These attractors of the system are demonstrated through the numerical simulations. The system exhibits the abundant dynamic properties of periodic orbit, quasi-periodic orbit, chaos and hyper-chaos, which is verified by calculating Lyapunov exponents and bifurcation diagrams. Spectral analysis shows that the proposed system has a broad frequency bandwidth. The system analog circuit can present periodic, chaotic and hyper-chaotic states by adjusting a resistance, consequently changing the value of the added negative feedback controller. The observation on an analog oscilloscope verifies the existence of various attractors at a physical level as shown in Fig. 11 and is the foundation of the application in some engineering fields such as communication security.

References

[1] Lorenz E N. 1963 *J. Atmos. Sci.* **20** 130
[2] Rössler O E 1979 *Phys. Lett. A* **71** 155
[3] Qi G Y, Chen G R, Du S Z, Chen Z Q and Yuan Z Z 2005 *Phys. Lett. A* **352** 295
[4] Qi G Y and Chen G R 2008 *Phys. Lett. A* **409** 423
[5] Chen G R and Ueta T 1999 *Int. J. Bifurc. Chaos* **9** 1465
[6] Lü J H and Chen G R 2002 *Int. J. Bifurc. Chaos* **12** 659
[7] Qi G Y, van Wyk B J and Wyk M A 2009 *Chaos, Solitons and Fractals* **40** 2016
[8] Wang Z H, Qi G Y, Sun Y X, van Wyk B J and van Wyk M A 2010 *Nonlinear Dyn.* **60** 443
[9] Wang F Z, Qi G Y, Chen Z Q and Yuan Z Z 2007 *Acta Phys. Sin.* **56** 3137 (in Chinese)
[10] Chen Z Q, Yang Y and Yuan Z Z 2008 *Chaos, Solitons and Fractals* **38** 1187
[11] Qi G Y, Chen G R, van Wyk M A, van Wyk B J and Zhang Y 2008 *Chaos, Solitons and Fractals* **38** 705
[12] Jia H Y, Chen Z Q and Qi G Y 2011 *Nonlinear Dyn.* **65** 131
[13] Jia H Y, Chen Z Q and Ye F 2011 *Acta Phys. Sin.* **60** 010203 (in Chinese)
[14] Wang Z H, Qi G Y, Sun Y X, van Wyk M A, van Wyk B J and Zhang Y 2009 *Int. J. Bifarc. Chaos* **19** 3841
[15] Wang J W and Chen A M 2010 *Chin. Phys. Lett.* **27** 110501
[16] Zhang W and Liao S K 2009 *J. Mech. Sci. Technol.* **23** 1058
[17] Li C L, Yu S M, Wei L L and Li Y S 2012 *Chin. Phys B* **21** 100507
[18] Wu W J and Chen Z Q 2011 *Nonlinear Dyn.* **60** 615
[19] Cang S J, Qi G Y and Chen Z Q 2010 *Nonlinear Dyn.* **59** 515
[20] Wu W J, Chen Z Q and Yuan Z Z 2010 *Int. J. Innov. Computing, Information & Control* **6** 307
[21] Jia H Y, Chen Z Q and Yuan Z Z 2010 *Chin. Phys B* **19** 020507
[22] Dong E Z, Chen Z Q, Chen Z P and Ni J Y 2012 *Chin. Phys B* **21** 030501
[23] Yu S M 2008 *Acta Phys. Sin.* **57** 3374 (in Chinese)
[24] Qi G Y, van Wyk M A, van Wyk B J and Chen G R 2007 *Phys. Lett. A* **372** 124
[25] Qi G Y, van Wyk M A, van Wyk B J and Zhang Y 2009 *Chaos, Solitons and Fractals* **40** 2544
[26] Cang S J, Chen Z Q and Yuan Z Z 2008 *Acta Phys. Sin.* **57** 1493 (in Chinese)
[27] Jia H Y, Chen Z Q and Yuan Z Z 2009 *Acta Phys. Sin.* **58** 4496 (in Chinese)
[28] Xue W, Guo Y L and Chen Z Q 2009 *Acta Phys. Sin.* **58** 8146 (in Chinese)
[29] Wang F Z, Qi G Y, Chen Z Q, Zhang Y H and Yuan Z Z 2006 *Acta Phys. Sin.* **55** 4005 (in Chinese)
[30] Xue W, Mu J J and Jia H Y 2010 *Proceedings of the Third Interational Workshop on Chaos–Fractal Theories and Applications*, October 29–31, 2010, Kunming, China, p. 197
[31] Li N, Sun H Y and Zhang Q L 2012 *Chin. Phys. B* **21** 010503
[32] Zhao H, Ma Y J, Liu S J, Gao S G and Zhong D 2011 *Chin. Phys. B* **20** 120501
[33] Ri I, Feng Y L, Yao Z H and Fan J 2011 *Chin. Phys B* **20** 120504
[34] Li Y, Zhang Z M and Tao Z J 2009 *Acta Phys. Sin.* **58** 6818 (in Chinese)
[35] Bao H M and Zhu Y S 2009 *Acta Electronica Sin.* **37** 1222
[36] Long, M and Peng F 2009 *Acta Electronica Sin.* **37** 79
[37] Wang Z, Huang X, Li Y X and Song X N 2013 *Chin. Phys B* **22** 010504
[38] Wiggins S 1990 *Introduction to Applied Nonlinear Dynamical Systems and Chaos* (New York: Springer-Verlag)